Measurements of entrainment by axisymmetrical turbulent jets

By F. P. RICOU† AND D. B. SPALDING

Mechanical Engineering Department, Imperial College of Science and Technology, London, S.W.7

(Received 23 November 1960)

A new technique is described for measuring the axial mass flow rate in the turbulent jet formed when a gas is injected into a reservoir of stagnant air at uniform pressure. The jet is surrounded by a porous-walled cylindrical chamber, and air is injected through the wall until the pressure in the chamber is uniform and atmospheric, a condition which is taken to signify that the 'entrainment appetite' of the jet is satisfied.

Measurements made with the apparatus have allowed the deduction of an entrainment law relating mass flow rate, jet momentum, axial distance and air density, regardless of the density of the injected gas, and including the effects of buoyancy. When the injected gas burns in the jet the entrainment rate is up to 30 % lower than when it does not.

1. Introduction

The problem

Several accounts are available (e.g. Schlichting 1955; Pai 1954) of the turbulent jet which results from the injection of a fluid through a nozzle into a large reservoir in which a second fluid is at rest. In the present paper, attention is concentrated on one property of the jet: the mass flow rate across a section at right angles to the jet axis. This quantity will be denoted by the symbol m; it may be related to the fluid velocity u in the axial direction, the fluid density ρ, and the radial distance y by

$$m = \int_0^\infty 2\pi \overline{\rho u} y \, dy, \tag{1}$$

where the over bar denotes a time-mean.

The mass flow rate m is known to increase with distance x from the nozzle. As a consequence, fluid from the surrounding reservoir is drawn radially inwards towards the jet across its conical surface; this process is known as entrainment. Entrainment is also important in many more practical situations; for example, it controls the flow patterns in combustion chambers and furnaces; it causes 'fire-storms' around large conflagrations; and many mixing devices of the chemical industry rely on entrainment for their effectiveness. If such processes are to be understood and controlled, the quantitative laws which govern the rate of entrainment, i.e. the quantity dm/dx, must be discovered.

† Now at the Laboratoires de Mécanique des Fluides, Université de Grenoble.

Dimensional analysis may be employed to show that, when the fluid density is uniform, when the Reynolds number is high and when the distance x is much larger than the diameter of the orifice, m is proportional to x. More precisely, it may be demonstrated that

$$\frac{m}{xM^{\frac{1}{2}}\rho_1^{\frac{1}{2}}} = K_1, \tag{2}$$

where M stands for the excess momentum flux of the jet, ρ_1 is the density of the surrounding fluid,† and K_1 is a numerical constant. Consideration of Newton's Second Law of Motion shows that, since the static pressure of the flow is uniform, M must have a value which is independent of x; it is most easily evaluated at the orifice, where the fluid has the uniform velocity u_0, from

$$M = M_0 \equiv \tfrac{1}{4}\pi d_0^2 \rho_0 u_0^2. \tag{3}$$

Here d_0 is the orifice diameter and ρ_0 the density of the injected fluid.

The numerical magnitude of K_1 can only be determined, in the present state of turbulence theory, by experimental means. Similarly, only experiment can show how equation (2) must be modified when the jet density is rendered non-uniform by a chemical reaction in the jet, or by the existence of a difference of value between ρ_0 and the density of the surrounding fluid, ρ_1.

Previous work

Numerous measurements have been made of the axial-velocity profiles, $u(y)$, in isothermal air jets (see, for example, the bibliography compiled by Krzywoblocki 1956). These data may be inserted in equation (1), from which the mass flow rate m can then be evaluated by numerical quadrature; this has been done by Grimmett (1948), Polomik (1948) and Voorheis & Howe (1939).

Many authors have avoided the numerical quadrature by assuming that the $u(y)$ profile has one of the forms which permit analytical integration; the velocity and radius scales appropriate to a given section are then determined from, say, the measured velocity on the axis, and the radius at which the measured velocity has half this value. The resulting values for m then depend to some extent on the profile-shape assumed.

Values for K_1 obtained in this way for isothermal air jets range from about 0·22 up to 0·404, according to the investigator. The highest value, due to Schlichting (1955), is obtained by fitting to the experimental data of Reichardt (1942) a particularly full-skirted 'theoretical' curve.

The reasons for the present uncertainty about the value of K_1 are of several kinds. They include the following:

(i) It is difficult to measure $\overline{\rho u}$ at large values of y where the velocities are small and the flow may be intermittent; the presence of y as a multiplier of u in equation (1) augments the influence of inaccuracies in this region.

(ii) The above difficulty is avoided if an analytical form is chosen for the velocity profile. This choice, on the other hand, entails uncertainty as to what is

† The subscripts to ρ in equations (2) and (3) are not needed in the present discussion, which presumes that ρ is uniform throughout; they are nevertheless inserted for use later in the paper.

the 'best' profile. Small differences in profile height at large y can greatly affect the value of m which is deduced.

(iii) Whichever of the above procedures is used, it is desirable that x should be many times greater than d_0. Since the dynamic head at a Pitot tube in the jet is proportional to $(d_0/x)^2$, limitations on manometer sensitivity make it difficult to work at axial distances much greater than five times the length of the potential core.

Outline of the present contribution

The above remarks show that a new method of measuring m is required, even for uniform-density flows. When jets with non-uniform density are to be studied, the case for a new method is stronger still; for a recourse to equation (1) would now necessitate measurement of a density profile as well as one of velocity, and would raise questions as to the relation of $\overline{\rho u}$ to the measured $\bar{\rho}$ and $\overline{\rho u^2}$.

The present paper reports a new experimental method which is not open to the objections mentioned above: m is measured more directly and simply; no integration is required. This technique is described in § 2 below.

The results of the study are presented in § 3 and figures 4, 5 and 7. Summarized briefly, they are: that K_1 is equal to 0·282; that equation (2) holds for non-uniform density without modification provided that buoyancy effects are negligible; and that the presence of combustion reduces K_1. The role of buoyancy is not so easily summarized; it is discussed in § 4.

2. Apparatus

The principle of the method

In the ideal free jet which is under consideration, the surrounding reservoir is large and, except in the vicinity of the jet axis, at uniform pressure; the entrained fluid flows radially inward towards the jet axis. If, however, a turbulent jet is partially enclosed by cylindrical walls, the radial inflow is impeded; the fluid entrained by the enclosed part of the jet has to flow axially in the annular space between the cylindrical wall and the conical 'boundary' of jet; the corresponding axial pressure gradients can be measured.

Now let us suppose that the cylindrical wall is made porous, and that a controlled and measured amount of fluid can be caused to flow through it in a radially inward direction. Then, if this flow is equal in quantity to that which would have passed through the area occupied by the wall if the wall had been absent, the axial pressure gradients referred to in the last paragraph will disappear.

This recognition underlies the experimental method which has been used: the flow rate through the porous wall is varied until no axial pressure gradients can be detected; this flow rate is then measured and presumed to be equal to that which would be entrained if the jet were unenclosed.

Details of the apparatus

Figure 1 shows the porous-walled chambers which were used. The axis of the jet is coincident with the axis of the cylindrical porous wall. The base of the cylinder was completely closed, apart from the orifice from which the jet origin-

ated, and the upper end of the resulting chamber was partially closed; these measures had the effect of augmenting the axial pressure gradients which prevailed when the flow through the porous wall was not 'right', while in no way interfering with the radially inward flow to the jet when it was entraining under free-jet conditions.

The porous cylinders were built up of fine-grade filter cloth on a rigid framework. A Roots-type blower was used to supply the entrainable air; this permitted the use of an appreciable pressure drop (up to 5 in. of water) across the porous cylinder and helped to ensure uniformity of inflow. Calibrated orifice plates were

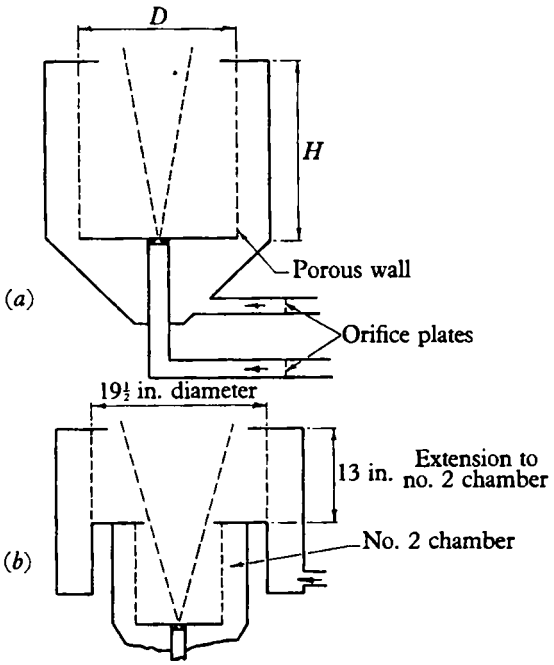

FIGURE 1. (*a*) Leading dimensions of three chambers.
(*b*) Dimensions of extension to no. 2 chamber.

	Entrainment chamber		
No.	1	2	3
H in.	8·7	13	3
D in.	5·8	8·9	8·9

used to measure the rate of supply of this air. The orifices used were of rounded profile, designed according to B.S. 1042. Their diameters (d_0) ranged from 0·0625 in. to 1·25 in. The corresponding range of dimensionless axial distances (x/d_0) over which measurements could be made was from 418 to 2·4.

The axial pressure difference which was measured was that across the outlet aperture; since the pressure variations within the chamber were small, this difference can be thought of as that between the pressure in the chamber and the pressure of the atmosphere. The micromanometer used was of the direct-reading type developed by Spalding (1950).

Preliminary tests: the choice of aperture size

The size of the aperture in the mask at the upper end of the 'entrainment chamber' had to be chosen with care. On the one hand, it was desired that the hole should be small, since this led to an easily detected pressure difference, when the flow through the porous wall was not properly matched to the free-jet requirements; however, if the hole were made too small, the mask would interfere with the axial flow in the jet itself.

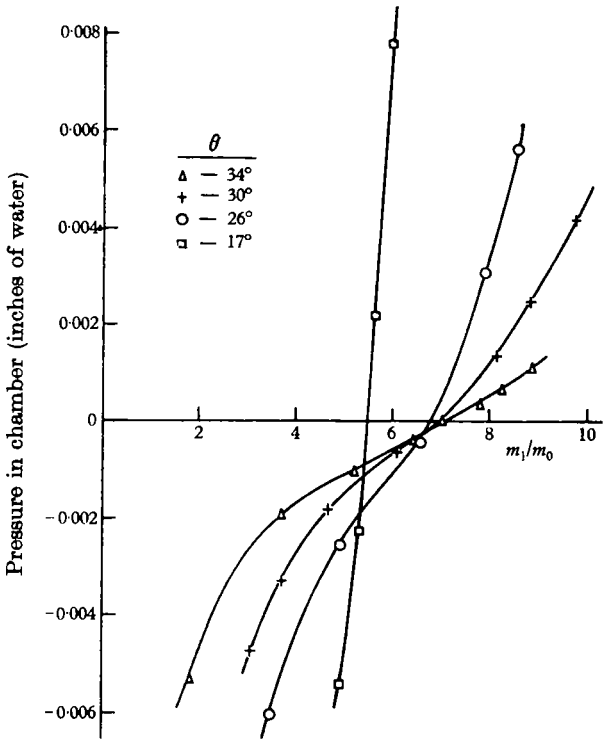

FIGURE 2. Variation of chamber pressure with flow rate through porous wall, for various apertures. Nozzle, 0·5 in. diameter; $x/d_0 = 25{\cdot}6$; $u_0 = 112$ ft./sec. (No. 2 chamber.)

Figure 2 shows the results of preliminary tests leading to the choice of aperture size, the latter being expressed in terms of the angle θ subtended by a diameter of the aperture at the centre of the base of the chamber. The ordinate is the excess pressure in the chamber; the abscissa is the ratio of the mass of air flowing through the porous wall, m_1, to the mass of gas (air) injected through the orifice, m_0; m_0, and the orifice diameter, d_0, have the same values throughout; each curve is drawn for a different value of aperture angle θ.

Inspection of figure 2 confirms that the smaller θ is the more steeply the excess pressure varies with variations of m_1; it also confirms that the aperture size influences the value of m_1/m_0 which gives zero excess pressure, if θ is too small. The latter influence is slight if θ is 30° or more; thus figure 2 shows that the value

of m_1/m_0 corresponding to free-jet conditions for the situation in question can be taken as 7·0. These tests led to the choice of 30° for the aperture angle in all the tests reported below.

Preliminary tests: the effect of the Reynolds number

Tests were carried out, using air as the injected fluid, to establish the value of the Reynolds number above which equation (2) was valid. Some of the data are recorded in figure 3 in the form of plots of m_1/m_0 versus the Reynolds number. The latter quantity is defined by

$$R \equiv \rho_0 u_0 d_0/\mu_0, \tag{4}$$

where μ_0 is the viscosity of the injected gas. From now onwards, m_1 will be used as signifying that value of the air flow rate through the porous wall which causes

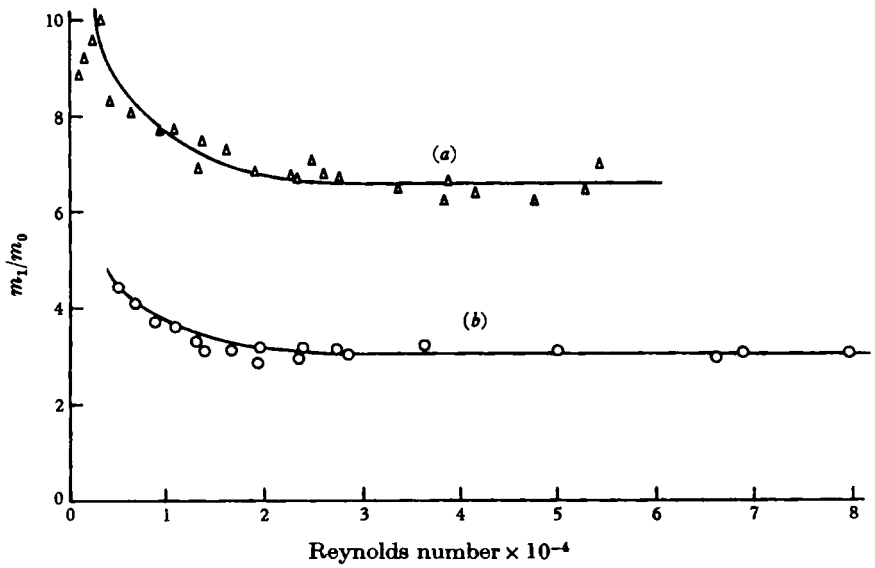

FIGURE 3. Variation of entrainment rate with the Reynolds number. (*a*) No. 2 chamber. Nozzle, 0·5 in. diameter; $x/d_0 = 25{\cdot}6$. (*b*) No. 1 chamber. Nozzle, 0·625 in. diameter; $x/d_0 = 13{\cdot}7$.

axial pressure gradients to disappear; m_1 is therefore connected with m, the mass flow rate in a free jet of length equal to the length of the entrainment chamber, by

$$m = m_1 + m_0. \tag{5}$$

The tests of figure 3 were carried out by varying the injection flow rate, and so the Reynolds number, and then measuring the corresponding m_1. Evidently, the ratio m_1/m_0 was approximately constant for Reynolds numbers in excess of $2{\cdot}5 \times 10^4$. All test data appearing in the remainder of the paper can be taken as pertaining to Reynolds numbers greater than this value, except for those in which the injected fluid is hydrogen.

3. Experimental results

Air into air: isothermal

Experiments were made with various combinations of chamber length x and nozzle diameter d_0, when the injected gas was air at the same temperature as the air supplied through the porous wall. The results are represented by the points in figure 4 clustered near the straight line marked (a); this line may be represented by the formula

$$\frac{m}{m_0} = 0{\cdot}32\frac{x}{d_0}. \tag{6}$$

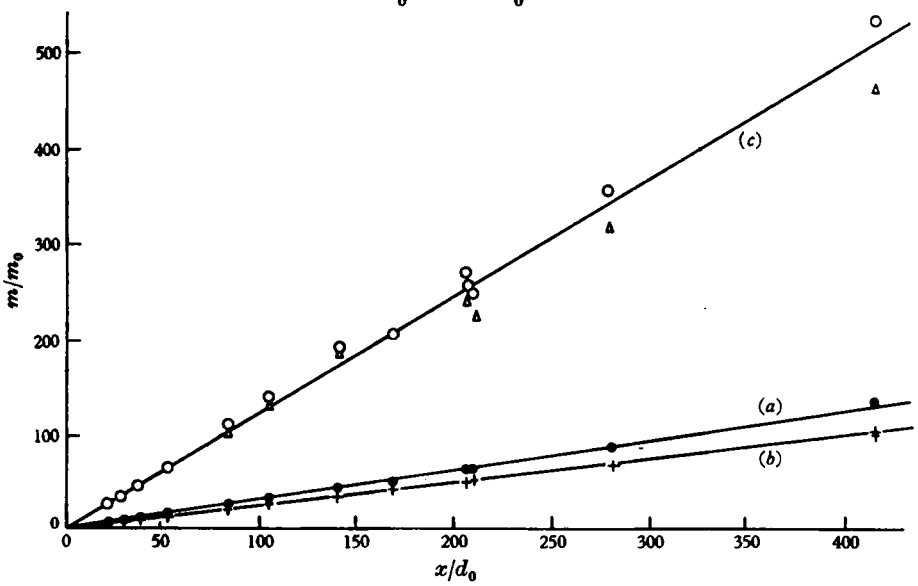

FIGURE 4. Variation of entrainment rate with axial distance for isothermal jets. Experimental results: (a) ●, air into air; (b) +, propane and carbon dioxide into air; (c) ○, hydrogen into air; (△, entrainment chamber inverted).

Heavy gas into air: isothermal

Corresponding measurements were made when the injected fluid was carbon dioxide or propane, two gases with equal densities, the temperatures being equal to that of the air supplied through the porous cylinder. The results are shown in figure 4 as a series of points clustered near the straight line marked (b): this line can be represented by the formula

$$\frac{m}{m_0} = 0{\cdot}26\frac{x}{d_0}. \tag{7}$$

Although flammable, the propane was not ignited in the experiments referred to here.

Light gas into air: isothermal

Figure 4 also contains results obtained by similar experiments in which hydrogen was the injected gas; the hydrogen jet was not ignited. The results are represented by the points near the straight line (c), the formula for which is

$$\frac{m}{m_0} = 1{\cdot}2\frac{x}{d_0}. \tag{8}$$

Since buoyancy was thought to affect the hydrogen jets, some experiments were carried out with the entrainment chamber inverted; it is seen that this inversion had an effect.

The high viscosity of hydrogen, and other limitations, prevented the performance of tests at Reynolds numbers in excess of 17,500.

Fuels into gas: combustion

Measurements were also made of the entrainment rate which prevailed when the fuel gases in the jet (propane and hydrogen) were ignited; in some cases both air and fuel were injected through the orifice simultaneously. The results of these tests, which showed a considerable effect of buoyancy, will be introduced in figure 7 below.

4. Discussion of results

Jets of uniform density

The equations (6), (7) and (8) may be cast in the form of equation (2) by introduction of equation (3) for the excess momentum flux and of a corresponding equation for the injected mass flux, m_0, namely

$$m_0 = \tfrac{1}{4}\pi d_0^2 \rho_0 u_0. \tag{9}$$

Equations (6), (7) and (8) then lead respectively to

$$\frac{m}{xM^{\frac{1}{2}}\rho_1^{\frac{1}{2}}} = 0{\cdot}32(\tfrac{1}{4}\pi)^{\frac{1}{2}} = 0{\cdot}283, \tag{10}$$

$$\frac{m}{xM^{\frac{1}{2}}\rho_1^{\frac{1}{2}}} = 0{\cdot}26(\tfrac{1}{4}\pi)^{\frac{1}{2}}(\tfrac{44}{29})^{\frac{1}{2}} = 0{\cdot}284, \tag{11}$$

$$\frac{m}{xM^{\frac{1}{2}}\rho_1^{\frac{1}{2}}} = 1{\cdot}2(\tfrac{1}{4}\pi)^{\frac{1}{2}}(\tfrac{2}{29})^{\frac{1}{2}} = 0{\cdot}279, \tag{12}$$

wherein $(\frac{44}{29})$ and $(\frac{2}{29})$ represent the density ratio ρ_0/ρ_1 for the respective cases of propane or carbon dioxide, and hydrogen.

Comparison of equations (10), (11) and (12) leads to the conclusion that equation (2) is valid, within the experimental error, for all the experimental results cited so far, if K_1 is given the value 0·282.

The same conclusion can be expressed differently by noting that all the data can be held to obey the relation

$$\frac{m}{m_0} = 0{\cdot}32\frac{x}{d_0}\left(\frac{\rho_1}{\rho_0}\right)^{\frac{1}{2}}. \tag{13}$$

This is illustrated by figure 5, which contains the data of figure 4 replotted in the manner indicated by equation (13).

The effect of buoyancy: theory

When the density of the fluid in the jet differs from that of the surrounding air, hydrostatic forces cause the excess momentum flux to increase with x (assuming that the jet fluid is the lighter and that the flow direction is upward). Consequently equation (2) no longer correctly expresses the variation of m with x.

Dimensional analysis indicates that, when x becomes very large, m is proportional to $x^{\frac{3}{2}}$ (Batchelor 1954); for this to hold, however, the excess momentum flux of the jet, M, must greatly exceed the value of M_0 defined by equation (3). How should m vary with x when M and M_0 are of the same order?

A tentative answer to this question may be obtained by supposing that the local rate of entrainment is uniquely related to the local excess momentum flux in accordance with the differential equation

$$\frac{1}{(M\rho_1)^{\frac{1}{2}}}\frac{dm}{dx} = 0{\cdot}282. \tag{14}$$

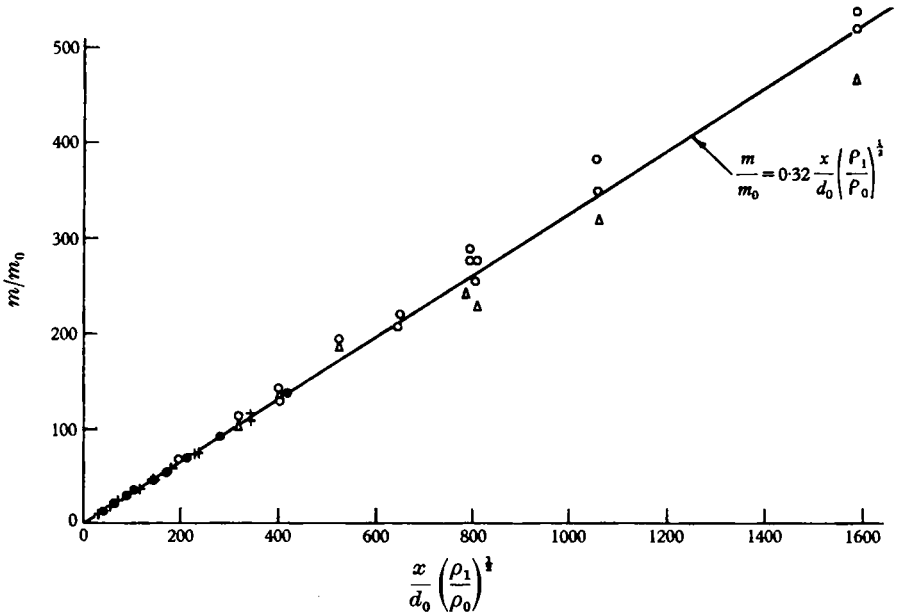

FIGURE 5. Entrainment rate for isothermal jets. Experimental results: (*a*) ●, air into air; (*b*) +, propane and carbon dioxide into air; (*c*), ○, hydrogen into air; (△, entrainment chamber inverted).

An assumption of this character has been made by Morton, Taylor & Turner (1950), and other authors, in connexion with the rise of turbulent plumes in the atmosphere.

In an unpublished study, one of the present authors has investigated the implications of equation (14), when combined with the assumptions: (i) that the velocity and temperature profiles are Gaussian, (ii) that the ratio of the widths of the temperature and velocity profiles is equal to 1·17 for all x, (iii) that chemical reaction is confined to regions of the jet which are much closer to the orifice than is the section x. The results of this study are represented by the curve of figure 6; the ordinate and abscissa quantities of this graph are self-explanatory apart from the Froude number, F, which is defined by:

in the absence of chemical reaction,

$$F \equiv \frac{c_1 T_1}{(h_0 - h_1)}\frac{u_0^2}{gd_0}\left(\frac{\rho_1}{\rho_0}\right)^{\frac{1}{2}}, \tag{15}$$

or, when chemical reaction occurs,

$$F \equiv \frac{c_1 T_1}{m_{fu} H + c_0 (T_0 - T_1)} \frac{u_0^2}{g d_0} \left(\frac{\rho_1}{\rho_0}\right)^{\frac{1}{2}}. \tag{16}$$

Here the symbols signify:

c	specific heat of gas at constant pressure,
T	absolute temperature of air,
h	enthalpy,
g	gravitational acceleration,
m_{fu}	mass fraction of fuel in injected gas,
H	heat of combustion of fuel,

and subscripts 0 and 1 refer, as before, to the injected fluid and to the surrounding air respectively.

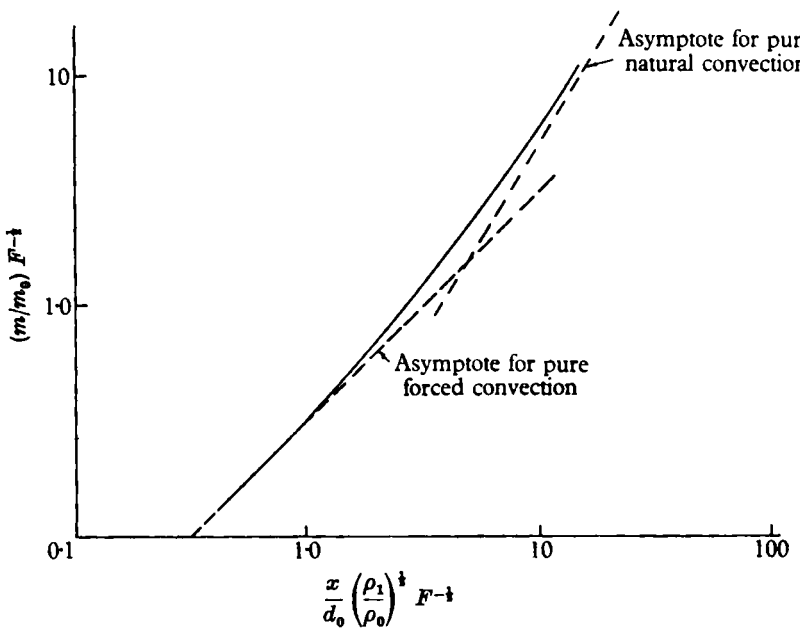

FIGURE 6. Theoretical prediction of entrainment in buoyant jets.

The effect of buoyancy: experiment

Figure 7 presents the data of figure 4 (upward flow only) together with the results of measurements made with burning jets. Also drawn for comparison is the curve of figure 6. The following features are evident.

(i) The data points lie close to the curve in the forced-convection régime; this, of course, is to be expected from figure 5, for example.

(ii) The influence of increasing buoyancy predicted by the theoretical curve, viz. an increased slope in the upper right corner, is exhibited by the experimental data. It is chiefly the hydrogen diffusion-flame data which are in question here.

(iii) Some of the data points, particularly those for pre-mixed hydrogen-air jets, lie well below both the curve and its forced-convection asymptote.

(iv) The scatter is considerable.

Comparison with previous work

It has already been stated that, in the absence of buoyancy, K_1 has been found by previous authors to lie between 0·22 and 0·404; the value obtained from the present work, viz. 0·282, can therefore be said to lie near the middle of the range of earlier values. The ease with which the measurements were made, in the present

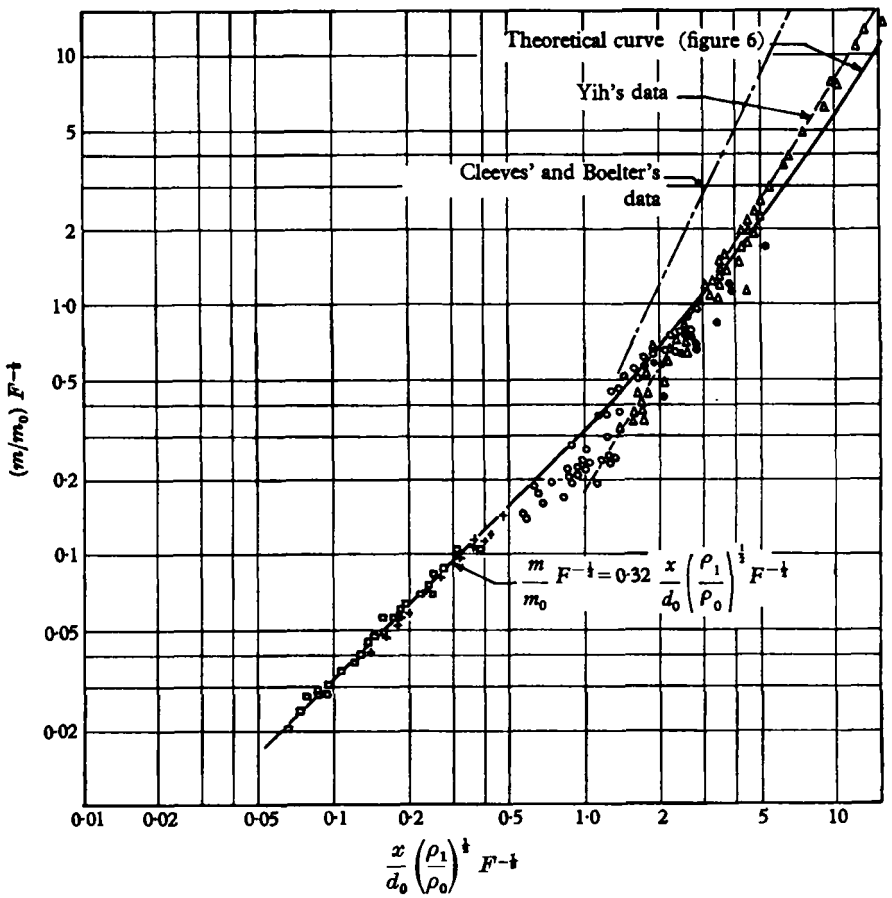

FIGURE 7. Entrainment by buoyant jets and flames. +, Unburnt propane jet; □, unburnt hydrogen jet; ○, pre-mixed air–hydrogen flame; △, hydrogen diffusion flame; ●, propane diffusion flame.

investigation, together with the straightforwardness of their interpretation, leads us to believe that the present value of K_1 is the most reliable established so far.

The finding that equation (2) holds, in the absence of buoyancy effects, for jets of non-uniform density was expected; it accords with the surmise of Squire & Trouncer (1944), and with the suggestion of Thring & Newby (1953), that the characteristic length of a turbulent jet is not d_0 but $d_0(\rho_0/\rho_1)^{\frac{1}{2}}$.

Other authors who have presented experimental data for the natural convection régime include Yih (1951), and Cleeves & Boelter (1947); the data of these authors are represented on figure 7 by broken straight lines which have been

plotted by ignoring experimental scatter and assuming Gaussian velocity and temperature profiles.

The data of Yih agree fairly well with the present hydrogen diffusion-flame data; both sets lie appreciably above the theoretical curve, indicating that the entrainment rate is greater in a buoyant jet than a non-buoyant one of the same excess momentum. The data of Cleeves & Boelter show the same tendency to an even more marked degree; they are, however, probably the least reliable of the data on figure 7, being appreciably influenced by potential-core effects.

5. Conclusions

(*a*) The new experimental technique for measuring the rate of entrainment by a turbulent jet was found to be easy to use, and to be applicable to jets of non-uniform density and to larger values of x/d_0 than had previously been investigated.

(*b*) The constant K_1 of equation (2) was found to have the value 0·282, irrespective of the density ratio.

(*c*) The curve of figure 6, based on the entrainment assumption expressed by equation (14), represents approximately the influence of buoyancy on the entrainment. However, it must be noted that: (i) there is a tendency for the curve to predict too low an entrainment rate in the natural-convection régime; (ii) the curve predicts too high an entrainment rate for some flames; (iii) the experimental scatter of the results of the present and earlier work in the natural-convection régime precludes the drawing of firm conclusions at present.

One of the authors (F. P. R.) acknowledges the financial support of the States of Jersey Committee of Education, and of Thomas Hedley and Company, Ltd.

This research was supported by a contract between Imperial College and the National Engineering Laboratory; the Director of the N.E.L. has given his permission for publication.

REFERENCES

Batchelor, G. K. 1954 *Quart. J. Roy. Met. Soc.* **80**, 339.

Cleeves, V. & Boelter, L. M. K. 1947 *Chem. Engng Progr.* **43**, 123.

Grimmett, H. L. 1948 M.S. Thesis, University of Illinois.

Krzywoblocki, M. Z. 1956 *Jet Prop.* **26**, 760.

Morton, B. R., Taylor, G. I. & Turner, J. S. 1950 *Proc. Roy. Soc.* A, **234**, 1.

Pai, S. I. 1954 *Fluid Dynamics of Jets.* New York: Van Nostrand.

Polomik, E. E. 1948 M.S. Thesis, University of Illinois.

Reichardt, H. 1942 *V.D.I.-Forschungsheft.* p. 414. (2nd ed. 1951).

Schlichting, H. 1955 *Boundary Layer Theory.* London: Pergamon Press.

Spalding, D. B. 1950 *J. Sci. Instrum.* **27**, 310.

Squire, H. B. & Trouncer, J. 1944 Round jets in a general stream. *Aero. Res. Counc. Tech. Rep.* R. &. M. no. 1974.

Thring, M. W. & Newby, M. P. 1953 *Fourth Symposium on Combustion*, p. 789. Baltimore: Williams and Wilkins.

Voorheis, T. S. & Howe, E. D. 1939 *Proc. Pac. Coast Gas Ass.* **30**, 198.

Yih, C. S. 1951 *Proc. First U.S. Nat. Congr. Appl. Mech.* p. 941.